QUARTERLY PROGRESS REPORT

[June 01 2018 - August 31 2018]

PROJECT TITLE: Landfill Leachate Pretreatment prior to Discharge to Sewer: Metal Recovery and Nitrogen Removal

PRINCIPAL INVESTIGATORS:
Youneng Tang, Ph.D., Assistant Professor
Department of Civil and Environmental Engineering, FAMU-FSU College of Engineering
2525 Pottsdamer Street Suite A130 Tallahassee FL 32310; Tel: 850-4106119; Fax: 850-4106142; ytang@eng.famu.fsu.edu

Gang Chen, Ph.D., P.E., Professor
Department of Civil and Environmental Engineering, FAMU-FSU College of Engineering
2525 Pottsdamer Street Suite A140 Tallahassee FL 32310; Tel: 850-4106303; Fax: 850-4106142; gchen@eng.famu.fsu.edu

PROJECT WEBSITE:
https://www.eng.famu.fsu.edu/~ytang/project7.html

Project summary: Leachates generated from most landfills in Florida are discharged to municipal wastewater treatment plants (WWTP). However, leachate is toxic to activated sludge when the concentrations of heavy metals are high. Additionally, leachate usually has high concentration of nitrogen, which may result in the discharge violation according to the Numeric Nutrient Criteria of Florida (Chapter 62-650, F.A.C.; Chapter 62-302, F.A.C.). Therefore, WWTP owners are becoming reluctant to accept landfill leachate without pretreatment. The objective of this proposal is to evaluate a potentially easy-to-implement, inexpensive, and sustainable onsite leachate pretreatment method for removing and recovering metals and making nitrogen easier to be removed in the WWTP. This method uses a submerged anaerobic bioreactor to pretreat the leachate prior to discharge to the WWTP. Metals are removed in the forms of metal sulfide precipitates in the bioreactor. Metal sulfides differ from each other in magnetic properties, which makes it possible for them to be separated by a magnetic separator and recovered as valuable resources. Some of the recalcitrant organic nitrogen is converted to bioavailable nitrogen through reactions in the anaerobic filter including hydrolysis, acidogenesis, and acetogenesis, which increase total nitrogen removal in the WWTP.

Work Accomplished during this Reporting Period:

Tasks 1 and 2 were completed in the first two quarters. In this quarter (the third quarter), we completed most of Tasks 3 and 4. We anticipate that we will complete all six tasks as scheduled by Nov 30, 2018.

At the end of this quarter, about 51% the total organic carbon (TOC) in the leachate was removed by the anaerobic bioreactor. Methane accounted for ~85% of the produced biogas, suggesting a high quality gas that could be reused. 75% of the iron (Fe) was removed. Fe speciation modeling suggests that the Fe removal was mainly due to the removal of fulvic acid, which released Fe from the Fe-fulvic acid complex, followed by precipitation of metal sulfides.

Task 3: Reactor operation and loading optimization

Materials and Methods

Reactor operation. Figure 1 is a photo of the submerged anaerobic bioreactor for leachate pretreatment. The reactor has been operated at a hydraulic retention time (HRT) of 4.5 days and room temperature for about 18 weeks after inoculation. ~20 mL of the leachate was taken from the leachate storage bottle in a refrigerator (1.6 °C) and pumped into the reactor through a syringe pump each day. The influent and effluent were sampled and stored in the refrigerator. The samples were characterized once per week since inoculation. The reactor performance will be continually monitored until steady state at which the chemical oxygen demand (COD), total organic carbon (TOC), acetate, and methane (CH_4) in the reactor effluent do not change significantly. Methods for the determination of these parameters were summarized in previous quarterly reports. Based on the data collected, the reactor is close to a steady state since these water quality parameters have not varied significantly in the past few weeks. We anticipate to optimize the reactor operation in the next quarter.

Figure 1. Submerged anaerobic reactor.

Water quality analysis. This section describes methods for organic matter measurement. Various carbon species in the system were quantified to understand how the organic matters were removed in the bioreactor. To understand the composition of the untreated leachate, dissolved organic carbon (DOC) in the reactor influent were characterized by humic substances (humic acid (HA) and fulvic acid (FA)) and non-humic substances (acetate and other non-humic substances). We expected that some DOC in the influent would be converted to 1) methane and carbon dioxide in the headspace of the syringe collecting the treated leachate, 2) biomass, 3) carbonate precipitate that mainly consisted of calcium carbonate ($CaCO_3$) and magnesium carbonate ($MgCO_3$), 4) dissolved carbonate species that included carbonate (CO_3^{2-}), bicarbonate (HCO_3^-), and carbonic acid (H_2CO_3(aq)). All of these parameters were measured or calculated in Weeks 5, 10 and 15. The method details are described below.

DOC and its composition. DOC in the reactor influent and effluent was measured following the persulfate-ultraviolent method in Rice (2012). Acetate was measured using ion chromatography (IC) (Dionex, Aquion, Thermo Scientific) following Rice (2012). Fractions of DOC, including HA, FA, and non-humic substances other than acetate, were measured following

the procedure in van Zomeren and Comans (2007). To precipitate HA from a water sample, hydrochloride acid (6 mol/L) was added to 10 mL of the filtered sample until pH was 1. After 24 hours, the suspension was centrifuged at 3000 rpm for 20 minutes to separate the precipitated HA from the supernatant. After decanting the supernatant to a 15-mL centrifuge tube that was used later for measurement of FA and non-humic substances, the precipitated HA was dissolved by 10 mL 1 mol/L potassium hydroxide and measured as dissolved organic carbon (DOC). FA in the supernatant was separated from the non-humic substances using a column containing 3 mL of prewashed Supelite DAX-8 resin (Supelco, Bellefonte, PA, USA), which adsorbed FA. The supernatant was pumped through the DAX-8 resin column followed by 10 mL of 0.1 mol/L hydrochloride acid at a rate of 6 mL/hr to wash the resin. Then, FA was desorbed from the DAX-8 resin by pumping 20 mL of 0.1 mol/L potassium hydroxide through the column at the same rate. The eluent as the FA fraction was collected and measured as DOC. Non-humic substances were calculated as the difference between the DOC and humic substances (HA and FA). The non-humic substances were further divided into acetate and other non-humic substances.

Effluent headspace gas and its composition. The treated leachate and produced gas were collected by a closed graduate syringe from which the headspace and leachate volumes were directly read. The headspace mainly contained methane (CH_4) and carbon dioxide (CO_2). The CH_4 concentration in the headspace was measured using gas chromatography (SRI Instruments). (Borges et al., 2011; Ozgur and Uysal, 2011). During the measurement, the column temperature was held at 50 ^oC for 3 minutes and then increased at a rate of 40 ^oC/min until 220 ^oC. The headspace gas volume and CH_4 concentration was then used to calculate the total methane mass in the syringe based on the Henry's law. The total methane mass was then divided by the effluent liquid volume to calculate the "assumed methane concentration in the effluent", which was later used for the carbon balance analysis in Figure 5. The carbon dioxide concentration in the headspace was estimated by assuming that all the rest of the headspace gas was CO_2. Ideal gas equation was applied to calculate the CO_2 mass, which was further used to calculate the "assumed CO_2 concentration in the effluent" by dividing the effluent leachate volume.

Biomass synthesis. The DOC used for biosynthesis in the anaerobic biological reactor can be estimated as (Ahmed and Lan, 2012; Canziani et al., 2006; Henze et al., 2001; Kennedy and Lentz, 2000; Rittman and McCarty, 2001):

$$Biomass(\frac{mg\ C}{L}) = Y \times (S^0 - S) \quad (1)$$

,where Y is the yield coefficient 0.024 mg C in cell/mg COD, S^0 is the COD in the influent, S is the COD in the effluent.

Dissolved inorganic carbon. The total dissolved inorganic carbon including carbonate, bicarbonate and carbonic acid was estimated for the reactor influent and effluent by Equation 2. The total inorganic carbon in the effluent was higher than that in the influent due to the biological conversion of organic carbon to inorganic carbon. The difference between the influent and effluent total dissolved inorganic carbon (after unit conversion from mol/L to mg C/L) represented the total dissolved inorganic carbon accumulation used in Figure 5. All the units in Equations 2 to 9 were mol/L.

$$\left[CO_3^{2-}\right]_{total} = \left[CO_3^{2-}\right] + \left[HCO_3^-\right] + \left[H_2CO_3(aq)\right] \quad (2)$$

,in which, the three carbonate species on the right side of the equation are further calculated based the following three equations, respectively,

$$\left[HCO_3^-\right] = Alkalinity - 2\left[CO_3^{2-}\right] - \left[OH^-\right] + \left[H^+\right] - \left[NH_3(aq)\right] - \left[CH_3COO^-\right] \quad (3)$$

$$[CO_3^{2-}] = [HCO_3^-] \times 10^{-10.3+pH} \quad (4)$$

$$[H_2CO_3(aq)] = [HCO_3^-] \times 10^{-pH+6.8} \quad (5)$$

In Equation 3, alkalinity was measured using the titration method (Rice et al., 2012), pH was measured using a multi-parameter meter (HQ440D, HACH) through the electrometric method (Rice et al., 2012), and then used to estimate $[H^+]$ and $[OH^-]$, $[NH_3(aq)]$ and $[CH_3COO^-]$ were calculated from Equations 6 and 7. Equations 3-5 were solved simultaneously to obtain $[HCO_3^-]$, $[CO_3^{2-}]$, and $[H_2CO_3\ (aq)]$.

$$[NH_3(aq)] = \frac{[NH_4^+]_{total}}{(1+10^{-pH+9.3})} \quad (6)$$

$$\left[CH_3COO^-\right] = \frac{\left[CH_3COO^-\right]_{total}}{(1+10^{-pH+4.7})} \quad (7)$$

, in which, $[NH_4^+]_{total}$ and $[CH_3COO^-]_{total}$ were measured using IC (Dionex, Aquion, Thermo Scientific).

For data quality control, two independent methods were used to calculate $[H_2CO_3(aq)]$ and the results were compared. One was based on Equation 5, and the other was based on Equation 8 based on the Henry's law, assuming the dissolved CO_2 in the leachate was in equilibrium with the headspace partial pressure of the CO_2.

$$[H_2CO_3(aq)] = [CO_2(g)] \times 0.031 \quad (8)$$

,in which, 0.031 is the Henry's law constant for CO_2 in the unit of mol/(L·atm) (Sander, 2015); $[CO_2\ (g)]$ is the gas pressure of CO_2 in the unit of atm; $[H_2CO_3\ (aq)]$ is in the unit of mol/L.

Precipitated carbon. It is assumed that carbon was precipitated mainly as $MgCO_3$ and $CaCO_3$ following Equation 9 and 10.

$$Mg^{2+} + CO_3^{2-} \rightarrow MgCO_3 \downarrow \quad (9)$$

$$Ca^{2+} + CO_3^{2-} \rightarrow CaCO_3 \downarrow \quad (10)$$

The molar concentration of the precipitated carbon associated with Mg and Ca were calculated as follows,

$$Carbon_{precipitated} = [Mg^{2+}]_{inf} - [Mg^{2+}]_{eff} + [Ca^{2+}]_{inf} - [Ca^{2+}]_{eff} \quad (11)$$

,in which, $[Mg^{2+}]_{inf}$ and $[Mg^{2+}]_{eff}$ the were molar concentration of magnesium in the influent and effluent, respectively, and $[Ca^{2+}]_{inf}$ and $[Ca^{2+}]_{eff}$ were the molar concentration of calcium in the influent and effluent, respectively. Dissolved calcium and magnesium concentrations in the influent and effluent were measured using a microwave plasma-atomic emission system (Agilent Technologies 4100) following the EPA method 3050B (EPA, 1996). The molar concentration was then converted to mass concentration of carbon to analyze the conversion of carbon species in Figure 5.

Results and Discussion

Organic matter removal performance overview. Figure 2 summarizes the organic matter removal in the reactor during the past 18 weeks, which can be divided into three phases. In Phase 1 (Week 1 - 8), the average acetate concentration increased from 1780 mg C/L in the influent to 2320 mg C/L in the effluent, and ammonium increased from 2250 mg N/L in the influent to 2520 mg N/L in the effluent (ammonium data will be presented in the next quarterly report along with other nitrogen species), suggesting the occurrence of hydrolysis, acidogenesis, and acetogenesis. Representative acetate and ammonium production reactions based on the three processes are summarized in Table 1. Phase 2 (Week 8 - 12) was a transition phase since 1) TOC and COD started to decrease, and 2) acetate started to be converted to methane. In Phase 3 (Week 12-18), all the four processes (hydrolysis, acidogenesis, acetogenesis and methanogenesis) occurred simultaneously. At the end of Phase 3, TOC decreased from 8170 mg C/L to 4020 mg C/L, and COD decreased from 24300 mg/L to 12600 mg/L. About 12.6% of TOC was converted to methane. The biogas (mainly CH_4 and CO_2) production rate reached 3.2 L gas/L leachate (See Figure 3) which is comparable to the literature (Bohdziewicz, et al., 2008). The CH_4 proportion reached 85% of the biogas (Figure 4), which was higher than the typical value 50-75% (Kim et al., 2003; Tanigawa, 2017; Vergara-Fernandez et al., 2008; Weiland, 2010), suggesting a very high quality biogas that could be reused. The high CH_4 concentration in the biogas could be due to the precipitation of significant inorganic carbon (See Week 15 data in Figure 5).

Insight into the organic matter removal. To gain more insight into the conversion of organic matters in the reactor, Figure 5 shows the carbon speciation at different phases. The influent stored in the refrigerator did not change significantly over the 18 weeks except for small conversion of FA to acetate. In Week 5 (Phase 1), the major reaction in the reactor was conversion of FA and non-humic substances other than acetate to acetate and CO_2: The FA decreased by 532 mg C/L and the non-humic substances other than acetate decreased by 121 mg C/L while acetate increased by 513 mg C/L and CO_2 in the gas increased to 300 mg C/L. The CO_2 concentration used here was an assumed value calculated by dividing the CO_2 mass in the headspace by the liquid volume.

In Week 10 (Phase 2), the major reaction in the reactor were the conversion of non-humic substances other than acetate (decreased from 1.18×10^3 mg C/L in the influent to 315 mg C/L in the effluent) and FA (decreased from 2.93×10^3 to 2.45×10^3 mg C/L) to CH_4 (increased from 0 in the influent to 444 mg C/L in the effluent), acetate (increased from 2.12×10^3 to 2.37×10^3 mg C/L), CO_2 (increased from 0 to 179 mg C/L), and biomass (increased by 150 mg C/L).

In Week 15 (Phase 3), the major reactions in the reactor were the conversion of acetate (decreased from 2.22×10^3 mg C/L in the influent to 950 mg C/L in the effluent), non-humic substances other than acetate (decreased from 1.28×10^3 to 99 mg C/L), and FA (decreased from 3.10×10^3 to 2.53×10^3 mg C/L) to CH_4 (increased from 0 in the influent to 1.03×10^3 mg C/L in the effluent), total dissolved inorganic carbon (increased by 991 mg C/L), CO_2 (increased from 0 to 428 mg C/L) and biomass (increased by 236 mg C/L). Inorganic carbon precipitation was observed in Phase 3, but not the other two phases probably due to the increased production of CO_2 (see Table 1), which provided CO_3^{2-} in the reactor to precipitate $CaCO_3$ and $MgCO_3$. The pH through the treatment was between 7.5 and 8.0 (Figure 6) probably due to the balance between organic acids production in hydrolysis, acidogenesis and acetogenesis and acetate consumption in methanogenesis (See Table 1).

For data quality control, the H_2CO_3(aq) concentration was calculated by two different methods that were based on two independently measured water quality parameters: One was

calculated by the alkalinity method in Equation 5 (33 mg C/L effluent) and the other by the Henry's law method in Equation 8 (36 mg C/L effluent). They were generally consistent. The total concentration of various carbon species in the influent was similar to the total concentration of carbon species in the effluent (See Figure 5), which approximately closed the carbon balance, and provided another line of evidence for the data quality control.

Table 1. Representative reactions at four stages during anaerobic digestion.

Process	Representative reactions
Hydrolysis	$C_6H_{10}O_4 + 2H_2O \rightarrow C_6H_{12}O_6 + H_2$
	$CH_3CH(CH_3)CH(NH_3^+)COO^- + 2H_2O \rightarrow (CH_3)_2CHCOO^- + NH_4^+ + CO_2 + 2H_2$
	$C_6H_{12}O_6 + 2H_2 \rightarrow 2CH_3CH_2COOH + 2H_2O$
Acidogenesis	$CH_3CH(OH)CH(NH_3^+)COO^- + H_2 \rightarrow CH_3COO^- + \frac{1}{2}CH_3(CH_2)_2COO^- + \frac{1}{2}H^+ + NH_4^+$
	$CH_3CH(CH_3)CH(NH_3^+)COO^- + 2H_2O \rightarrow (CH_3)_2CHCOO^- + NH_4^+ + CO_2 + 2H_2$
	$C_6H_{12}O_6 \rightarrow 3CH_3COOH$
	$CH_3CH_2OH + H_2O \rightarrow CH_3COO^- + H^+ + 2H_2$
Acetogenesis	$CH_3CH_2COO^- + 3H_2O \rightarrow CH_3COO^- + HCO_3^- + H^+ + 3H_2$
	$CH_3CH_2CH_2COO^- + 2H_2O \rightarrow 2CH_3COO^- + H^+ + 2H_2$
	$CH_3COO^- + H^+ \rightarrow CH_4 + CO_2$
Methanogenesis	$H_2 + \frac{1}{2}CO_2 \rightarrow \frac{1}{4}CH_4 + \frac{1}{2}H_2O$

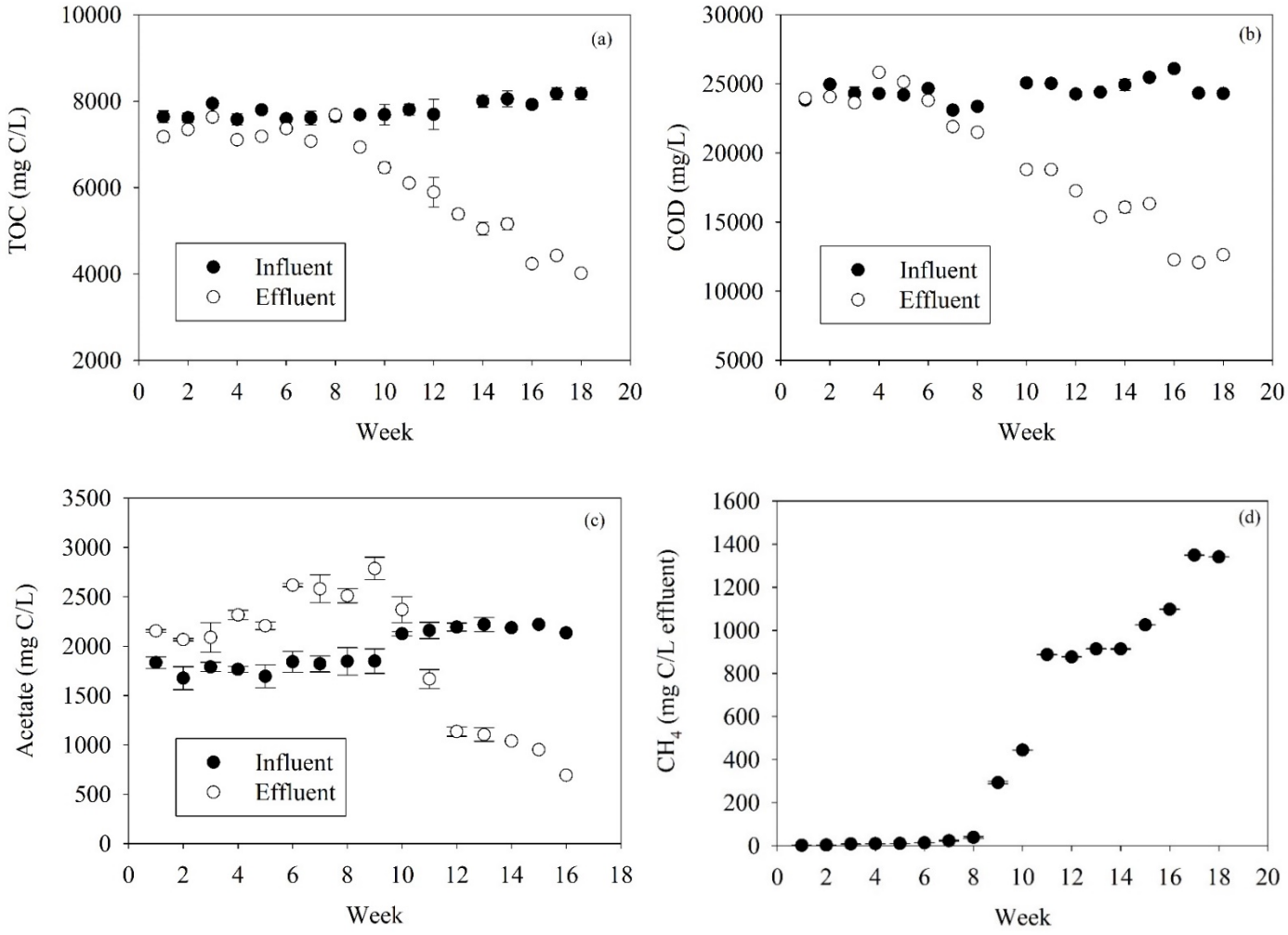

Figure 2. Weekly measured parameters including (a) TOC, (b) COD, (c) acetate and (d) CH_4. Note: The CH_4 concentration in panel was the "assumed methane concentration in the effluent", which was the total methane mass in the syringe that collected the treated leachate and gas divided by the effluent liquid volume.

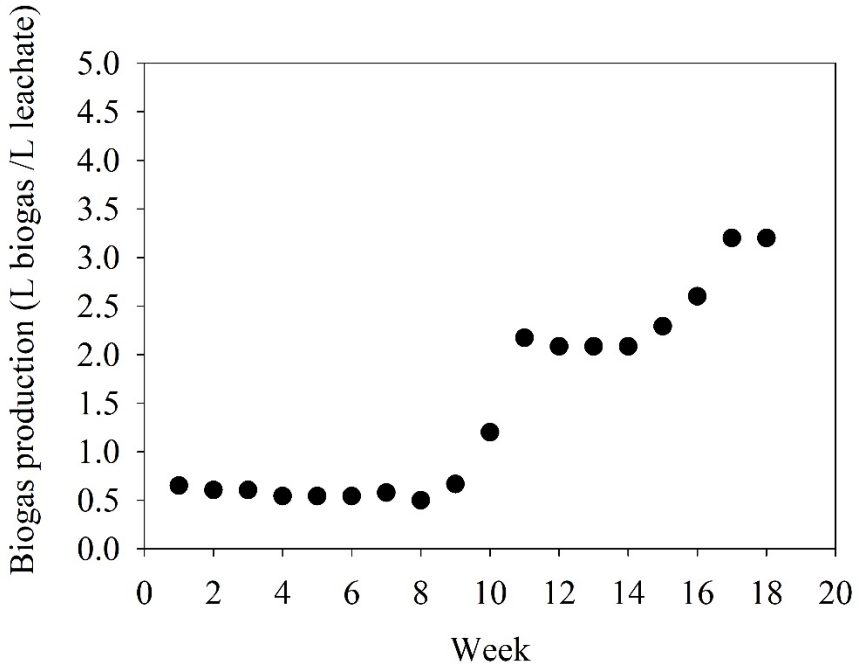

Figure 3. Biogas production rate.

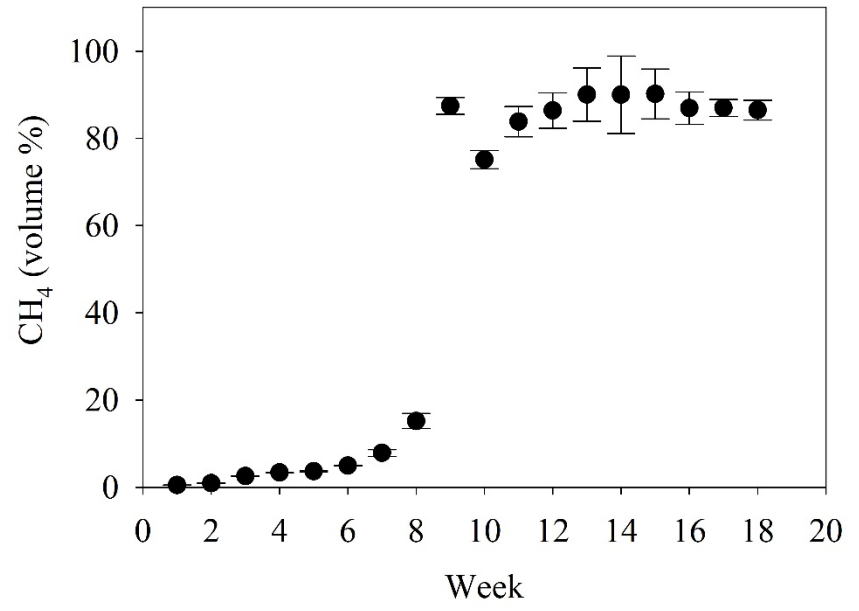

Figure 4. Methane volume percentage in the biogas (syringe headspace).

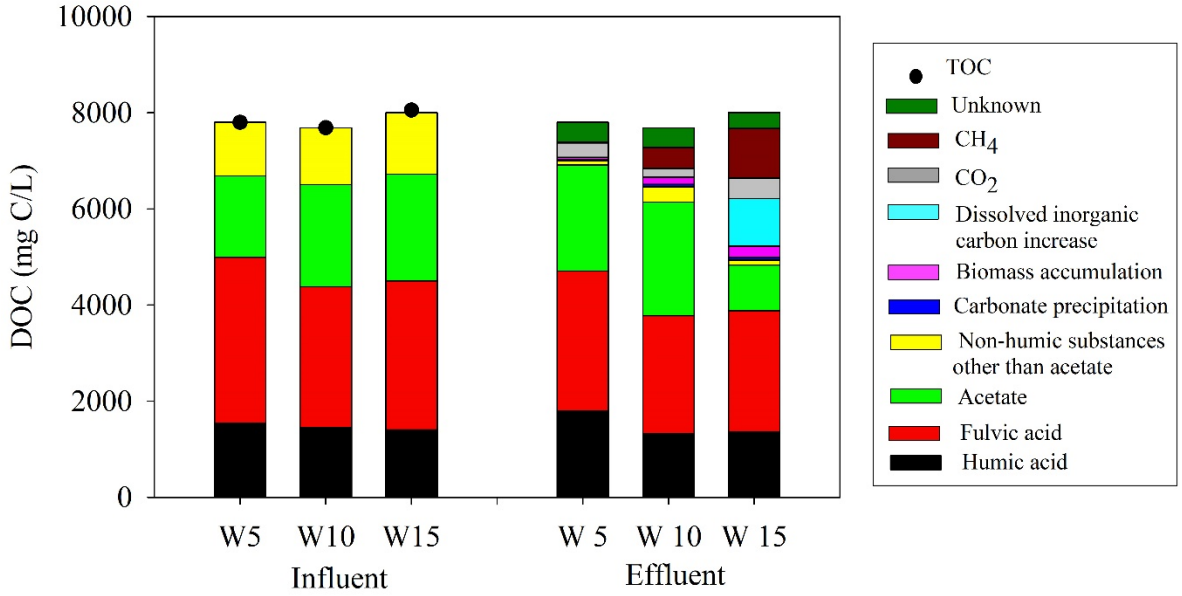

Figure 5. Carbon speciation in the anaerobic reactor. W = Week

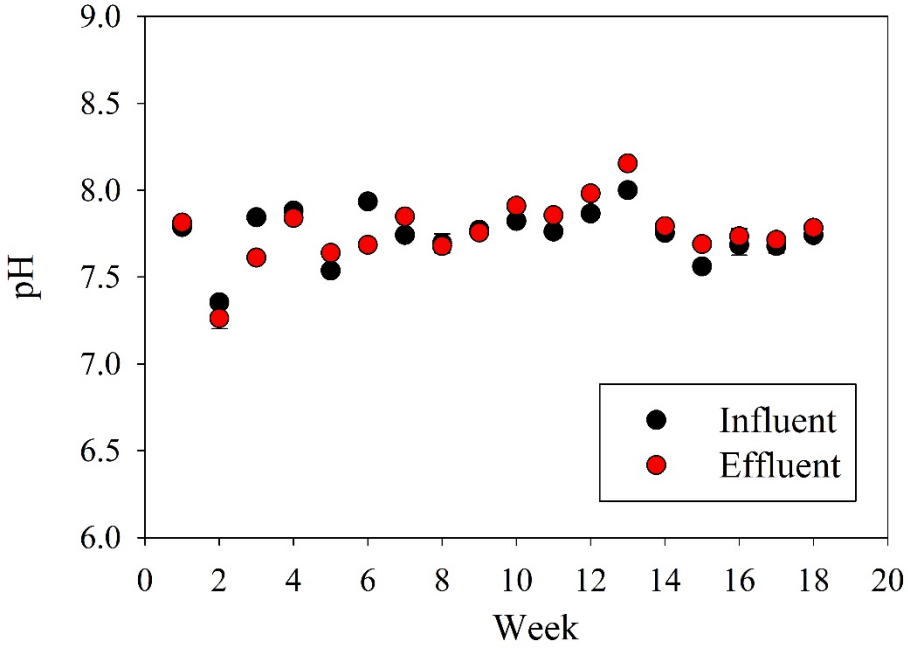

Figure 6. pH in the reactor influent and effluent.

Task 4: Metal speciation modeling

Experiments

The total metal and total dissolved metal were measured according to the EPA method 3050 B using a microwave plasma-atomic emission system (MP-AES) (Agilent Technologies 4100). The metals investigated in this study included Fe, Pb, and Ni since their concentrations exceeded at least one of the local sewer discharge standards in Florida (see previous quarterly reports #1 and 2). As shown in Figure 7, 75% of Fe was removed but the removal of Pb and Ni was negligible. Starting on Week 8, some dissolved Fe was converted to particulate Fe probably due to the formation of iron crystals during leachate storage, which is further discussed below in the modeling section. The majority of the total dissolved Fe in the reactor influent and effluent was in the form of organic metal complex (91-96%, See Figure 8). All of the iron species decreased in the reactor effluent compared to the influent.

The removal of Fe was probably due to the formation of iron sulfide precipitate, which is further discussed in the modeling section below. Sulfate concentration was reduced from 120 mg S/L to less than 20 µg S/L (the quantification limit) throughout the experiment (Figure 9). To understand how sulfate reduction to sulfide affected the metal removal and precipitation, the hydrogen sulfide species were measured or calculated as follows. The hydrogen sulfide in the headspace, $H_2S(g)$, of the leachate storage bottle and the syringe for collecting the effluent was measured using a portable hydrogen sulfide analyzer (Jerome 631-X): <0.01 mg/L for the storage bottle headspace and 0.982 mg/L for the syringe headspace. Sulfide species in the liquid phase were calculated using Equations 12 to 14 according to the Henry's law (Sander, 2015):

$$[H_2S(aq)] = [H_2S(g)] \times 0.11 \quad (12)$$

$$[HS^-] = \left[H_2S(aq)\right] \times 10^{-6.96+pH} \quad (13)$$

$$[S^{2-}] = [HS^-] \times 10^{-7.21+pH} \quad (14)$$

,in which, $[H_2S\ (aq)]$, $[HS^-]$ and $[S^{2-}]$ were the concentrations of the dissolved sulfide species in the liquid and had unit of mol/L. The total liquid sulfide species ($[S^{2-}]_{total}$) in the influent and effluent were calculated in Equation 15:

$$[S^{2-}]_{total} = [H_2S(aq)] + [HS^-] + [S^{2-}] \quad (15)$$

The $[S^{2-}]_{total}$ in the influent and effluent were 0 and 2.12 mg S/L respectively.

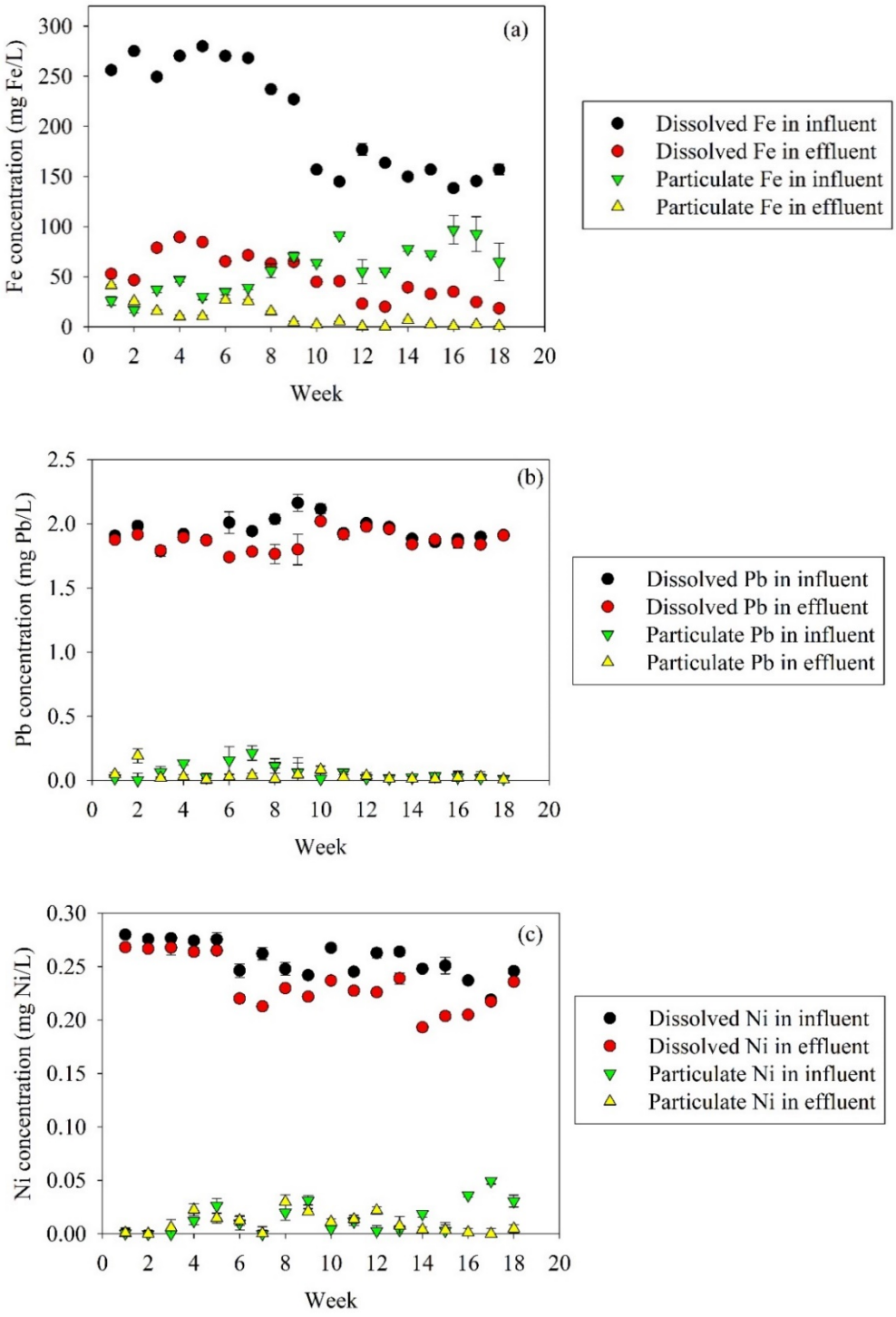

Figure 7. The dissolved and particulate metal concentrations of (a) Fe, (b) Pb and (c) Ni in the bioreactor influent and effluent.

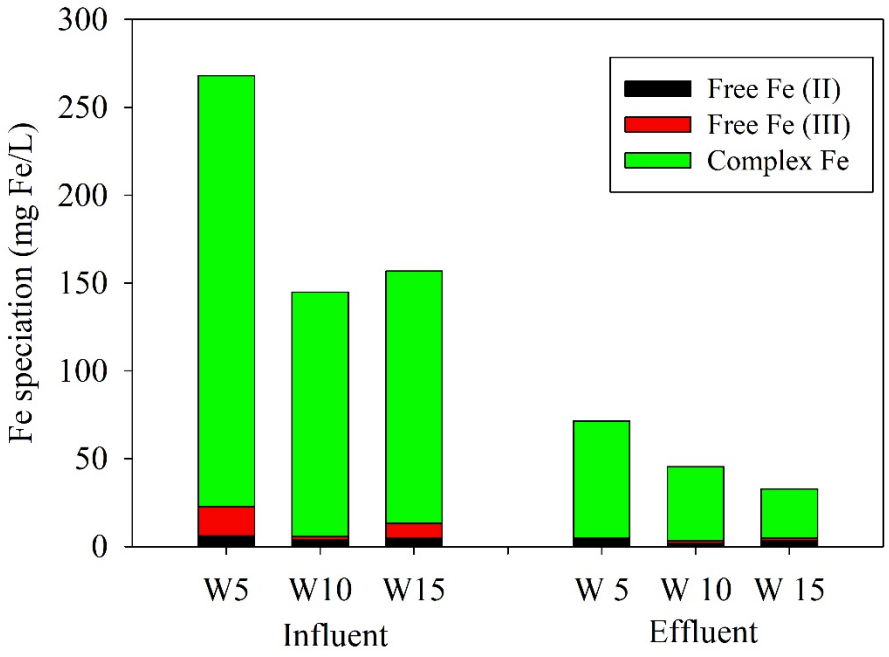

Figure 8. The measured Fe species in different phases.

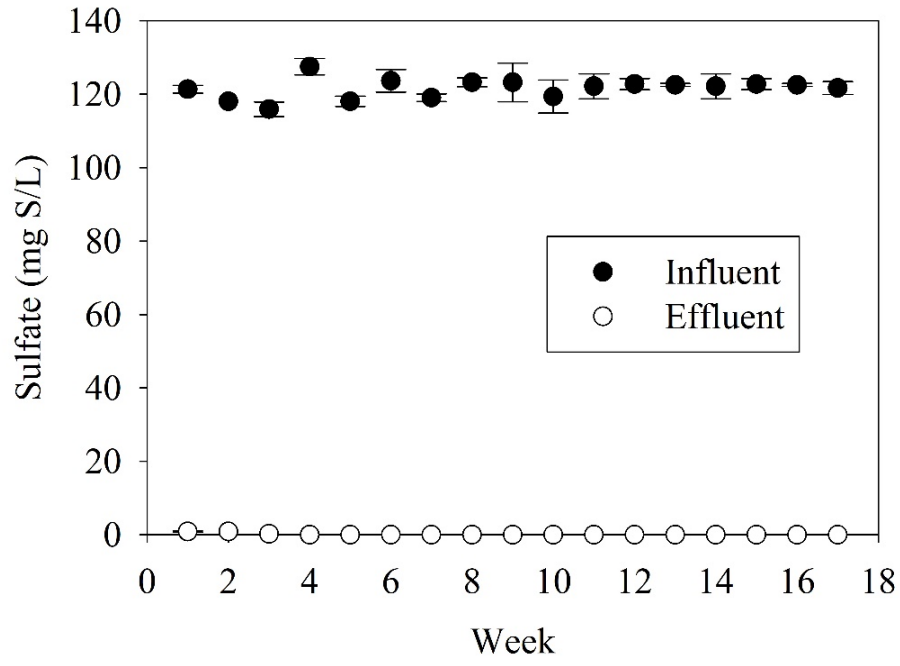

Figure 9. Sulfate concentration in the reactor influent and effluent.

Modeling

To further understand the fate of the investigated metals in the bioreactor, the dissolved metal speciation in the influent and effluent was simulated using VISUAL MINTEQ, software for equilibrium speciation model development (Cloutier-Hurteau et al., 2007). The influent and effluent in Week 15 were chosen to be modeled. Stockholm Humic Model (SHM) was used for modeling organic matter complexation with metals. SHM uses a discrete site distribution assumption to describe proton and metal binding by humic substances, and assumes that the strong acid site proportion is higher in FA than that in HA (Gustafsson, 2001). The model input (See Table 2) included the total dissolved concentrations of metals including Fe, Ni, Pb, Zn, Cu, Ca, Mg, Na and K, total ammonium (*i.e.*, [NH_4^+] and [NH_3 (aq)]), total acetate (*i.e.*, [CH_3COO^-] and [CH_3COOH (aq)]), total dissolved inorganic carbon (sum of CO_3^{2-}, HCO_3^- and H_2CO_3), and total sulfide. It also included major anions (*i.e.*, chloride and sulfate), HA, FA, pH, and redox potential (Eh). The HA and FA concentration were calculated based on the carbon content in humic substances and typical chemical formula of HA ($C_9H_9NO_6$) and FA ($C_{14}H_{12}O_8$) (National Center for Biotechnology Information, 2018).

Table 2. Input for the influent and effluent models.

Species	Influent	Effluent
FA (mg FA/L)	5.69×10^3	3.24×10^3
HA (mg HA/L)	2.95×10^3	2.85×10^3
Total Dissolved Fe (mg Fe/L)	157	33
Total Dissolved Ni (mg Ni/L)	0.25	0.20
Total Dissolved Pb (mg Pb/L)	1.88	1.84
Total Dissolved Zn (mg Zn/L)	1.9	0.4
Total Dissolved Cu (mg Cu/L)	0.3	0.3
Total Dissolved Ca (mg Ca/L)	184	37
Total Dissolved Mg (mg Mg/L)	159	128
Total Dissolved Na (mg Na/L)	524	521
Total Dissolved K (mg K/L)	1.39×10^3	1.32×10^3
Total Ammonium (mg N/L)	2.30×10^3	2.65×10^3
Total Acetate (mg C/L)	2.22×10^3	9.50×10^2
Chloride (mg Cl/L)	4.00×10^3	3.89×10^3
Sulfate (mg S/L)	130	0
Total Sulfide (mg S/L)	0	2.1
Total Dissolved Inorganic Carbon (mg C/L)	1.08×10^3	2.08×10^3
Eh (mV)	-153	-290
pH	7.56	7.69

The Fe speciation modeling results are summarized in Figure 10 and compared to the measured ion species concentrations in Table 3. The model and experiments were generally consistent for the free Fe (II) and Fe complex, but different for the free Fe (III) probably because some free Fe (II) was oxidized to Fe (III) during the measurement.

The effluent mainly differed from the influent in two ways per the modeling results in Figure 10. First, Fe (III) existed in the influent (accounting for 10% of the total dissolved Fe) mainly in the form of Fe (III)-FA complex and Fe (III)-HA complex, but almost completely disappeared in the effluent. The main cause was 1) the conversion of FA to products like acetate

and methane, which released Fe (III) as free Fe (III) and 2) the higher reducing environment in the effluent (*i.e.*, lower Eh in Table 2) compared to the influent, which reduced Fe (III) to Fe (II). Second, a higher percentage of Fe (II) was complexed with FA than HA in the influent due to the higher FA concentration and stronger acid sites in FA, but this trend changed in the effluent because of the removal of FA.

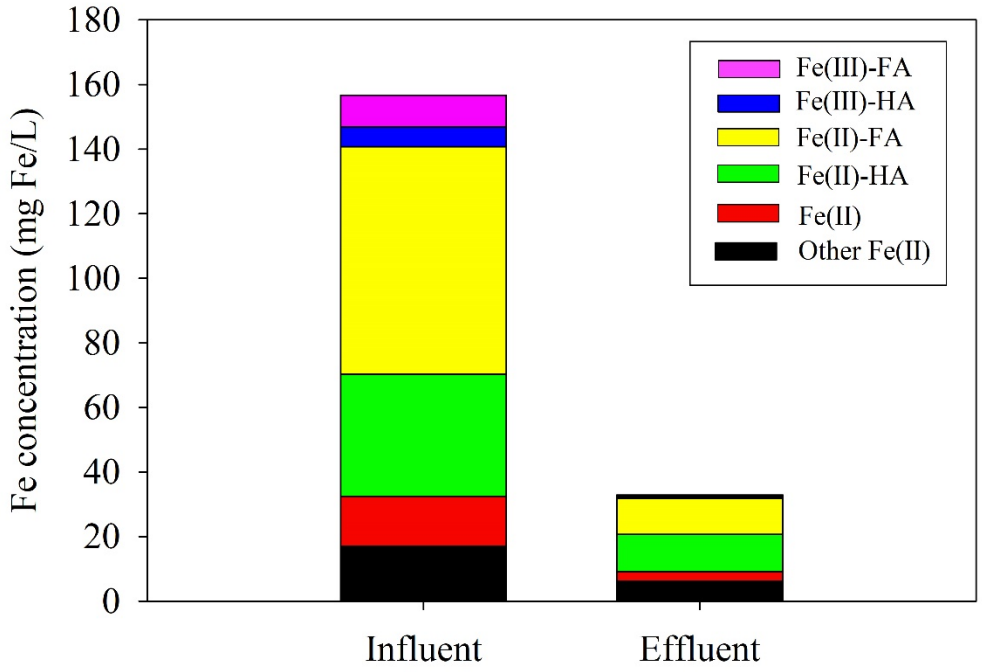

Figure 10. Modeled Fe speciation in the reactor influent and effluent at Week 15. Note: HA is humic acid and FA is fulvic acid. Other Fe (II) are Fe (II) complex with chloride, ammonia and bicarbonate et al.

Table 3. Fe concentration comparison between the model output and the experimental data.

	Influent		Effluent	
	Model	Experiment	Model	Experiment
Free Fe(II) (mg Fe/L)	15.5	4.67	2.97	3.47
Free Fe(III) (mg Fe/L)	1.70E-14	8.57	1.63E-17	1.38
Fe Complex (mg Fe/L)	142	144	29.8	27.9

VISUAL MINTEQ output saturation index of 24 Fe-containing minerals, 24 Pb-containing minerals, 9 Ni-containing minerals, and 57 minerals containing other metals for the influent and the effluent. Out of these minerals, 16 were summarized in Table 4 since they contained at least one of the three metals we focused on (*i.e.*, Fe, Pb, and Ni), and the saturation index was positive in the influent, effluent, or both. The 16 minerals included 13 Fe-containing minerals, two Ni-containing minerals, and one Pb-containing minerals; this comparison explained why the Fe removal was much higher than the Pb and Ni removal.

Table 4. Saturation index of possible common minerals.

Minerals	Chemical Formula	Influent	Effluent
Chalcopyrite	$CuFeS_2$	0.75	21.9
Cupric ferrite	$CuFe_2O_4$	2.91	-3.50
Akaganéite	$Fe(OH)_{2.7}Cl_{0.3}(s)$	3.39	0.72
Ferrihydrite (aged)	$Fe_2O_3 \cdot 0.5H_2O$	0.26	-2.38
Iron sulfide	FeS	-10.3	0.63
Greigite	$Fe(II)Fe(III)_2S_4$	-351	4.70
Goethite	alpha-FeO(OH)	2.46	-0.18
Hematite	Fe_2O_3	7.33	2.05
Lepidocrocite	gama-FeO(OH)	1.58	-1.06
Mackinawite	FeS	-9.64	1.28
Magnetite	$Fe(II)Fe(III)_2O_4$	13.5	7.79
Pyrite	FeS2	-9.08	8.88
Siderite	FeCO3	2.52	2.24
Nickel Sulfide (beta)	beta-NiS	-6.18	5.22
Nickel Sulfide (gamma)	gamma-NiS	-4.48	6.92
Galena	PbS	-4.84	6.07

Reference:

Ahmed, F. N.; Lan, C. Q. Treatment of landfill leachate using membrane bioreactors: A review. *Desalination,* **2012**, 287, 41-54.

Bohdziewicz, J.; Neczaj, E.; Kwarciak, A. Landfill leachate treatment by means of anaerobic membrane bioreactor. *Desalination*, **2008**, 221, 559-565.

Brandisheep, A.; Gebhardt, N. A.; Thauer, R. K.; Widdel, F.; Pfennig, N. Anaerobic acetate oxidation to CO_2 by Desulfobacter-Postgatei .1. Demonstration of all enzymes required for the operation of the citric-acid cycle. *Archives of Microbiology*, **1983**, 136, 222-229.

Borges, A.V.; Abril, G.; Delille, B.; Descy, J.P.; Darchambeau, F. Diffusive methane emissions to the atmosphere from lake Kivu (Eastern Africa). *Journal of Geophysical Research*, **2011**, 116, 1-7.

Canziani, R.; Emondi, V.; Garavaglia, M.; Malpei, F.; Pasinetti, E.; Buttliglieri, G. Effect of oxygen concentration on biological nitrification and microbial kinetics in a cross-flow membrane bioreactor (MBR) and moving-bed biofilm reactor (MBBR) treating old landfill leachate. *Journal of Membrane Science*, **2006**, 286, 202-212.

Chen, Y.; Cheng, J.J.; Creamer, K.S. Inhibition of anaerobic digestion process: A Review. *Bioresoure Techonology*, **2008**, 99(10), 4044-4064.

Cloutier-Hurteau, B.; Sauvé, S.; Courchesne, F. Comparing WHAM 6 and MINEQL+ 4.5 for the chemical speciation of Cu^{2+} in the rhizosphere of forest soils. *Environmental Science & Technology*, **2007**, 41 (23), 8104-8110.

Cresson, R.; Carrere, H.; Delgenes, J. P.; Bernet, N. Biofilm formation during the start-up period of an anaerobic biofilm reactor - Impact of nutrient complementation. *Biochemical Engineering Journal*, **2006**, 30, 55-62.

Cresson, R.; Escudie, R.; Steyer, J. P.; Delgenes, J. P.; Bernet, N. Competition between planktonic and fixed microorganisms during the start-up of methanogenic biofilm reactors. *Water Research*, **2008**, 42, 792-800.

Gustafsson, J.P. Modeling the acid-base properties and metal complexation of humic substances with the Stockholm Humic Model, *Journal of Colloid and Interface Science*, **2001**, 244, 102-112.

Henry, J. G.; Prasad, D.; Young, H. Removal of organics from leachates by anaerobic filter, *Water Research*, **1987**, 21, 1395-1399.

Henze, M.; Harremoes, P.; la Cour Jansen, J.; Arvin, E. Wastewater treatment: biological and chemical processes, *Springer Science & Business Media*, **2001**.

Henze, M.; VanLoosdrecht, M. C. M.; Ekama, G. A.; Brdjanovic, D. Biological wastewater treatment: Principles, modelling and design. *Cambridge University Press*, **2008**, 1-511.

Kennedy, E. J.; Lentz, E. M. Treatment of landfill leachate using sequencing batch and continuous flow upflow anaerobic sludge blanket (UASB) reactors. *Water Research*, **2000**, 34, 3640-3656.

Kim, J.; Park Ch.; Kim, T-H.; Lee, M.; Kim, S.; Kim, S-W.; Lee, J. Effects of various pretreatments for enhanced anaerobic digestion with waste activated sludge. *Journal of Bioscience and Bioengineering*, **2003**, 95(3), 2721-275.

Li, Y.; Lam, S.; Fang, H.H.P. Interactions between methanogenic, sulfate-reducing and syntrophic acetogenic bacteria in the anaerobic degradation of benzoate, *Water Research*, **1996**, 30(7), 1555-1562.

Middleton, A. C.; Lawrence, A. W. Kinetics of microbial sulfate reduction. *Journal of Water Pollution Control Federation*, **1977**, 49, 1659-1670.

Mizuno, O.; Li, Y.Y.; Noike, T., The behavior of sulfate-reducing bacteria in acidogenic phase of anaerobic digestion. *Water Research*, **1998**, 32(5), 1626-1634.

National Center for Biotechonology Information. https://www.ncbi.nlm.nih.gov/. **2018**.

Ozgur, D. O.; Uysal, Z., Hydrogen production by aqueous phase catalytic reforming of glycerine, *Biomass and Bioenergy*, **2011**, 35(2), 822-826.

Rittman, B.; McCarty, P. Environmental biotechnology: principles and applications. *McCraw-Hill. Inc., USA*, **2001**, 6-11.

Rice, E. W.; Baird, R. B.; Eaton, A. D.; Clesceri, L. S. *Standard Methods for the Examination of Water and Wastewater, 22nd Ed.*, **2012**.

Sander, R. Compilation of Henry's law constants (version 4.0) for water as solvent. *Atmospheric Chemistry and Physics*, **2015**, 15, 4399-4981.

Shinozuka, T.; Shibata, M.; Yamaguchi, T. Molecular Weight Characterization of Humic Substances by MALDI-TOF-MS. *Journal of the Mass Spectrometry Society of Japan*, **2004**, 52, 29-32.

Sun, J.; Hu, S. H.; Sharma, K. R.; Ni, B. J.; Yuan, Z. G. Stratified microbial structure and activity in sulfide- and methane-producing anaerobic sewer biofilms. *Applied and Environmental Microbiology*, **2014**, 80, 7042-7052.

Tanigawa, S., Biogas: Converting waste to energy. *Environmental and Energy Study Institute*, **2017**.

U.S. EPA. METHOD 3050B. Acid Digestion of Sediments, Sludges, and Soils. **1996**. https://www.epa.gov/sites/production/files/2015-06/documents/epa-3050b.pdf

Vergara-Fernandez, A.; Vargas, G.; Alarcon, N.; Velasco, A. Evaluation of marine algae as a source of biogas in a two-stage anaerobic reactor system. *Bioimass and Bioenergy*, **2008**, 32(4), 338-344.

Wang, Z.; Banks, C.J., Treatment of a high-strength sulphate-rich alkaline leachate using an anaerobic filter. *Waste Management*, **2007**, 27, 359-366.

Weiland, P., Biogas production: current state and perspectives. *Applied Microbiology and Biotechnology*, **2010**, 85(4), 849-860.

Widdel, F.; Pfennig, N. A new anaerobic, sporing, acetate-oxidizing, sulfate-reducing bacterium, Desulfotomaculum (emend.) acetoxidans. *Archives of Microbiology*, **1977**, 112, 119-22.

Wong, B.T.; Show, K.Y.; Lee, D.J.; Lai, J.Y., Carbon balance of anaerobic granulation process: Carbon credit. *Bioresource Technology*, **2009**, 100(5), 1734-1739.

Metrics:

1. List research publications resulting from this Hinkley Center project.
   None.

2. List research presentations resulting from this Hinkley Center project.
   1) Grant, A. and Acosta, J. Removal of organics from landfill leachate using anaerobic filter. Program of Excellence in STEM, Florida Agricultural and Mechanical University, Tallahassee, Jun. 28, 2018.

3. List who has referenced or cited your publications from this project?
   None.

4. How have the research results from this Hinkley Center project been leveraged to secure additional research funding?
   The PI is forming a team to apply for landfill research funds from the National Academies' Gulf Research Program.

5. What new collaborations were initiated based on this Hinkley Center project?
   The PI is collaborating with Geosyntec to submit a landfill research proposal to the *Environmental Research & Education Foundation.*

6. How have the results from this Hinkley Center funded project been used (will be used) by the FDEP or other stakeholders? (1 paragraph maximum)
   Will be discussed in the final report.

Pictures:

1). Lab work picture: Measurement of methane by Adrian Grant and Jerimiah Acosta (scholars from the Program of Excellence in STEM at Florida A&M University)

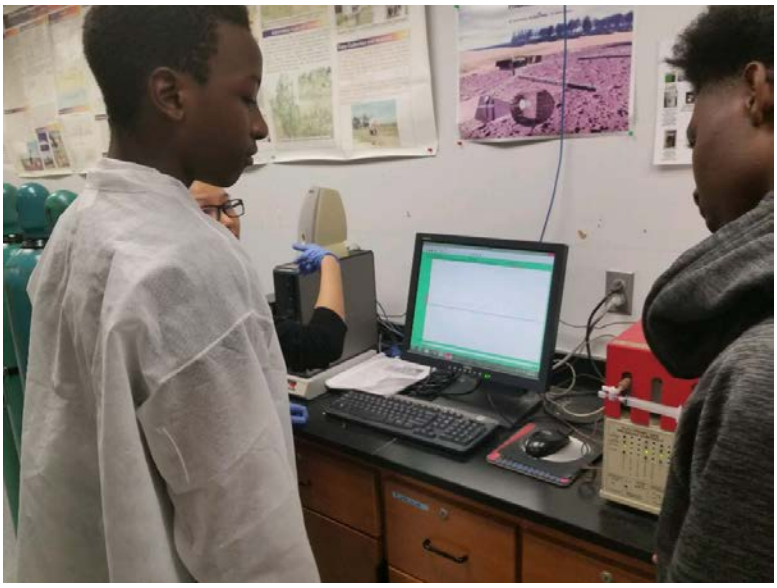

2). Poster presentation pictures: poster presentation by Adrian Grant and Jerimiah Acosta (scholars from the Program of Excellence in STEM at Florida A&M University)